Weak lensing of the primary CMB bispectrum

Asantha Cooray, Devdeep Sarkar, and Paolo Serra

Center for Cosmology, Department of Physics and Astronomy, University of California, Irvine, California 92697, USA

(Received 28 March 2008; published 17 June 2008)

The bispectrum of cosmic microwave background (CMB) anisotropies is a well-known probe of the non-Gaussianity of primordial perturbations. Just as the intervening large-scale structure modifies the CMB angular power spectrum through weak gravitational lensing, the CMB primary bispectrum generated at the last scattering surface is also modified by lensing. We discuss the lensing modification to the CMB bispectrum and show that lensing leads to an overall decrease in the amplitude of the primary bispectrum at multipoles of interest between 100 and 2000 through additional smoothing introduced by lensing. Since weak lensing is not accounted for in current estimators of the primordial non-Gaussianity parameter, the existing measurements of $f_{\rm NL}$ of the local model with WMAP out to $l_{\rm max} \sim 750$ is biased low by about 6%. For a high resolution experiment such as Planck, the lensing modification to the bispectrum must be properly included when attempting to estimate the primordial non-Gaussianity or the bias will be at the level of 30%. For Planck, weak lensing increases the minimum detectable value for the non-Gaussianity parameter of the local type $f_{\rm NL}$ to 7 from the previous estimate of about 5 without lensing. The minimum detectable value of $f_{\rm NL}$ for a cosmic variance limited experiment is also increased from less than 3 to $\sim$5.

DOI: 10.1103/PhysRevD.77.123006 PACS numbers: 98.70.Vc, 95.85.Sz, 98.65.Dx, 98.80.Cq

I. INTRODUCTION

The weak lensing of cosmic microwave background (CMB) anisotropy angular power spectrum is now well understood in the literature [1,2]. The modifications result in a smoothing of the acoustic peak structure at large angular scales and an increase in power below a few arcminute angular scales corresponding to the damping tail of CMB anisotropies [3].

The angular power spectrum of the lensing potential out to the last scattering surface can be established with quadratic estimators that probe lensing non-Gaussianity at the 4-point level of a CMB map [4]. Such a reconstruction of the lensing potential is helpful for CMB B-mode studies of polarization [5], especially in the context of searching for the signature of the primordial tensor modes [6]. This is due to the fact that in addition to inflationary gravitational waves, the B-modes of CMB polarization also contains a signal generated by lensing of scalar E-modes with a peak in power at a few arcminute angular scales [7]. The lensing reconstruction has now been applied to existing Wilkinson Microwave Anisotropy Probe (WMAP) data leading to a $\sim 2\sigma$ to 3σ detection of gravitational lensing in the CMB through a correlation between the reconstructed lensing potential and tracers of the large-scale structure such as radio galaxies [8,9].

In parallel with the progress on lensing studies with the CMB, the search for primordial non-Gaussianity using the CMB bispectrum with constraints on the non-Gaussianity parameter $f_{\rm NL}$ is now an active topic in cosmology [10–12]. The 5-year WMAP data is consistent with $-9 < f_{\rm NL} < 111$ at the 95% confidence level for the local model [13], though a nonzero detection of primordial non-Gaussianity at the same 95% confidence level with $26.9 < f_{\rm NL} < 146.7$ is claimed elsewhere using the WMAP 3-year data [14]. This result, if correct, has significant cosmological implications since the expected value under standard inflationary models is $f_{\rm NL} \lesssim 1$ [15–22], though alternative models of inflation, such as the ekpyrotic cosmology [23,24], generally predict a large primordial non-Gaussianity with $f_{\rm NL}$ at few tens.

Just as the CMB power spectrum is modified by lensing from potential fluctuations of the intervening large-scale structure [1], the CMB bispectrum will also be modified by gravitational lensing. The correlation between the projected lensing potential and CMB secondary effects, such as the integrated Sachs-Wolfe (ISW) effect or the Sunyaev-Zel'dovich (SZ) effect, leads to a non-Gaussian signal at the three-point level [25,26]. These secondary non-Gaussianities are expected even if the primordial perturbations are Gaussian and impact existing primordial non-Gaussianity parameter measurements by introducing a small, but unavoidable, bias [27–29].

Beyond secondary non-Gaussianities, weak lensing by the intervening large-scale maps the intrinsically non-Gaussian CMB sky to a different anisotropy pattern when observed today. Thus the bispectrum one reconstructs with a CMB map, assuming it to be of the expected form at the last-scattering surface due to primordial non-Gaussian perturbations, will result in a biased estimate of the primordial non-Gaussianity parameter. The existing estimator can be modified to account for lensing modifications and to obtain a bias-free estimate of the non-Gaussianity, but at the expense of factorizability that has allowed fast computation of the bispectrum in existing analyses [30]. Since

lensing modifies the anisotropy pattern by smoothing the fluctuations, a change in the minimum detectable non-Gaussianity parameter $f_{\rm NL}$ for a given experiment is expected to be different from the existing values in the literature [10].

In this paper, we present a general derivation of the lensed CMB primary bispectrum and quantify above statements on the changes imposed by lensing for the detection of primordial non-Gaussianity. We find that the non-Gaussianity parameter measured with WMAP, ignoring lensing, will result in an estimate of $f_{\rm NL}$ for the local model that is biased low by about 6%, when measurements are extended out to $l_{\rm max} \sim 750$. Furthermore, with lensing, the minimum detectable level of $f_{\rm NL}$ with Planck is increased by roughly 40% from less than 5 to about 7 and the cosmic variance limit of $f_{\rm NL}$ is increased from 3 to 5.

This paper is organized as follows: we first discuss the CMB primary bispectrum of the local type in Sec. II. Some basic ingredients related to the lensing calculation is presented in Sec. III. We derive the lensing effect on the bispectrum, under both flat-sky and all-sky formulations, in Sec. IV. We discuss our results and conclude with a summary in Sec. V. In illustrating our results we make use of the standard flat ΛCDM cosmological model consistent with WMAP with $\Omega_b = 0.042$, $\Omega_c = 0.238$, $h = 0.732$, $n_s = 0.958$, and $\tau = 0.089$.

II. CMB PRIMARY BISPECTRUM

The CMB temperature perturbation on the sky, $\Theta(\hat{\mathbf{n}}) = \Delta T(\hat{\mathbf{n}})/T$, is decomposed into its multipole moments

$$\Theta(\hat{\mathbf{n}}) = \sum_{lm} \Theta_{lm} Y_l^m(\hat{\mathbf{n}}). \tag{1}$$

The angular power spectrum and bispectrum of CMB anisotropies are defined in the usual way, respectively, as

$$\begin{aligned} \langle \Theta_{lm} \Theta_{l'm'} \rangle &= \delta_{l,l'} \delta_{m,m'} C_l^{\Theta\Theta}, \\ \langle \Theta_{l_1 m_1} \Theta_{l_2 m_2} \Theta_{l_3 m_3} \rangle &= \begin{pmatrix} l_1 & l_2 & l_3 \\ m_1 & m_2 & m_3 \end{pmatrix} B_{l_1 l_2 l_3}, \end{aligned} \tag{2}$$

where, for the bispectrum, we have introduced the Wigner-3j symbol (see the Appendix of Ref. [26] for some useful properties of this symbol).

The CMB bispectrum is generated by a coupling of the local-type with a quadratic correction to the Newtonian curvature such that

$$\Phi(\mathbf{x}) = \Phi_L(\mathbf{x}) + f_{\rm NL}[\Phi_L^2(\mathbf{x}) - \langle \Phi_L^2(\mathbf{x}) \rangle] \tag{3}$$

where $\Phi_L(\mathbf{x})$ is the linear and Gaussian perturbation and $f_{\rm NL}$ in the non-Gaussianity parameter, which is taken to be scale independent [10].

In Fourier space, we can decompose Eq. (3) as

$$\Phi(\mathbf{k}) = \Phi_L(\mathbf{k}) + f_{\rm NL} \Phi_{\rm NL}(\mathbf{k}), \tag{4}$$

with

$$\begin{aligned} \Phi_{\rm NL}(\mathbf{k}) = & \int \frac{d^3\mathbf{k}_1}{(2\pi)^3} \Phi_L(\mathbf{k} + \mathbf{k}_1) \Phi_L^*(\mathbf{k}_1) - (2\pi)^3 \delta(\mathbf{k}) \\ & \times \int \frac{d^3\mathbf{k}_1}{(2\pi)^3} P_\Phi(k_1), \end{aligned} \tag{5}$$

where $P_\Phi(k)$ is the linear power spectrum, defined as

$$\langle \Phi(\mathbf{k}) \Phi(\mathbf{k}') \rangle = (2\pi)^3 \delta(\mathbf{k} + \mathbf{k}') P_\Phi(k). \tag{6}$$

The multipole moments of the anisotropy can be written as

$$\Theta_{lm} = 4\pi (-i)^l \int \frac{d^3\mathbf{k}}{(2\pi)^3} \Phi(\mathbf{k}) g_{Tl}(k) Y_{lm}^*(\hat{\mathbf{k}}), \tag{7}$$

where $\Phi(\mathbf{k})$ from above is the primordial curvature perturbation in the Fourier space, and $g_{Tl}(k)$ is the radiation transfer function. With $\Phi_L(\mathbf{k})$ and $\Phi_{\rm NL}$, the moments can be separated into two components with $\Theta_{lm} = \Theta_{lm}^L + \Theta_{lm}^{NL}$.

The CMB angular power spectrum can be defined using the transfer function and the power spectrum of dominant linear fluctuations as

$$C_l^\Theta = \frac{2}{\pi} \int_0^\infty k^2 dk P_\Phi(k) g_{Tl}^2(k). \tag{8}$$

Using the definition of the angular bispectrum [Eq. (2)], the primordial temperature anisotropy bispectrum can be written as

$$\begin{aligned} B_{l_1 l_2 l_3} = & \sum_{m_1 m_2 m_3} \begin{pmatrix} l_1 & l_2 & l_3 \\ m_1 & m_2 & m_3 \end{pmatrix} [\langle \Theta_{l_1 m_1}^L \Theta_{l_2 m_2}^L \Theta_{l_3 m_3}^{NL} \rangle \\ & + \langle \Theta_{l_1 m_1}^L \Theta_{l_2 m_2}^{NL} \Theta_{l_3 m_3}^L \rangle + \langle \Theta_{l_1 m_1}^{NL} \Theta_{l_2 m_2}^L \Theta_{l_3 m_3}^L \rangle], \end{aligned} \tag{9}$$

which can be simplified to [10]

$$\begin{aligned} B_{l_1 l_2 l_3} = & 2 \mathcal{G}_{l_1 l_2 l_3} \int_0^\infty r^2 dr b_{l_1}^L(r) b_{l_2}^L(r) b_{l_3}^{NL}(r) \\ & + b_{l_1}^L(r) b_{l_2}^{NL}(r) b_{l_3}^L(r) + b_{l_1}^{NL}(r) b_{l_2}^L(r) b_{l_3}^L(r), \end{aligned} \tag{10}$$

where

$$b_l^L(r) = \frac{2}{\pi} \int_0^\infty k^2 dk P_\Phi(k) g_{Tl}(k) j_l(kr), \tag{11}$$

$$b_l^{\rm NL}(r) = f_{\rm NL} \frac{2}{\pi} \int_0^\infty k^2 dk g_{Tl}(k) j_l(kr), \tag{12}$$

and

$$\mathcal{G}_{l_1 l_2 l_3} = \sqrt{\frac{(2l_1 + 1)(2l_2 + 1)(2l_3 + 1)}{4\pi}} \begin{pmatrix} l_1 & l_2 & l_3 \\ 0 & 0 & 0 \end{pmatrix}. \tag{13}$$

When illustrating our results, we make use of a modified code of CMBFAST [31] for the standard flat ΛCDM cosmo-

logical model to fully calculate radiation transfer functions when generating the CMB primary bispectrum.

III. WEAK LENSING BASICS

The effects of weak lensing can be encapsulated, under the Born approximation, in the radial projection of the gravitational potential (Φ), given as [32]

$$\phi(\hat{\mathbf{n}}) = -2\int_0^{r_s} dr' \frac{d_A(r_s - r')}{d_A(r_s)d_A(r')}\Phi(\mathbf{r}(\hat{\mathbf{n}}), r'), \tag{14}$$

where $r(z)$ is the line-of-sight comoving distance (or look-back time) to a redshift z from the observer with last scattering surface at $r_s = r(z = 1100)$, and $d_A(r)$ is the comoving angular diameter distance. In a spatially flat universe, $d_A \rightarrow r$. Here, we ignore the time-delay effect as it is small compared to the geometric lensing effect captured by Eq. (14) [33].

The calculation related to the CMB bispectrum described below requires the angular power spectrum of lensing potential ϕ, which can be decomposed into the multiple moments as

$$\phi(\hat{\mathbf{n}}) = \sum_{lm} \phi_{lm} Y_l^m(\hat{\mathbf{n}}), \tag{15}$$

with the lensing power spectrum defined using $\langle \phi_{lm}\phi_{l'm'}\rangle = \delta_{l,l'}\delta_{m,m'}C_l^\phi$ to obtain [3]

$$C_l^\phi = \frac{2}{\pi}\int k^2 dk P_\Phi(k)[I_l^{\rm len}(k)]^2, \tag{16}$$

where

$$I_l^{\rm len}(k) = \int dr W^{\rm len}(r) j_l(kr),$$
$$W^{\rm len}(r) = -2F(r)\frac{d_A(r_s - r)}{d_A(r)d_A(r_s)}. \tag{17}$$

Here $F(r)$ describes the radial evolution of potential fluctuations. Modifications to the CMB anisotropies, generated at higher order in lensing potential fluctuations, are at the level of at most 5% relative to those due to the lensing potential angular power spectrum [34]. The bispectrum of lensing potentials, due to the nonlinear evolution of density perturbations, also modifies the CMB primary bispectrum, but these changes can also be ignored since the lensing potential bispectrum is at the order $(C_l^\phi)^2$, while changes we describe are first order in the angular power spectrum of the lensing potential. Using the Limber approximation, Eq. (16) can be further simplified, but we do not make use of this approximation in numerical calculations illustrated here since the flat-sky form of the potential power spectrum is known to bias lensing results of the power spectrum by about 10% at all multipoles [3].

IV. LENSING OF THE CMB BISPECTRUM

We first give a treatment of the lensing of the CMB bispectrum assuming a flat-sky approximation and discuss a derivation under the spherical sky later.

A. Flat-sky case

Weak lensing deflects the path of background photons resulting in a remapping of the observed anisotropy pattern on the sky. Following an approach similar to [3], we write the lensed temperature anisotropy as

$$\begin{aligned}\tilde{\Theta}(\hat{\mathbf{n}}) &= \Theta[\hat{\mathbf{n}} + \nabla\phi(\hat{\mathbf{n}})] \\ &\approx \Theta(\hat{\mathbf{n}}) + \nabla_i\phi(\hat{\mathbf{n}})\nabla^i\Theta(\hat{\mathbf{n}}) \\ &\quad + \tfrac{1}{2}\nabla_i\phi(\hat{\mathbf{n}})\nabla_j\phi(\hat{\mathbf{n}})\nabla^i\nabla^j\Theta(\hat{\mathbf{n}}) + \ldots\end{aligned} \tag{18}$$

Here, $\Theta(\hat{\mathbf{n}})$ is the unlensed CMB temperature anisotropy, $\tilde{\Theta}(\hat{\mathbf{n}})$ is the lensed anisotropy, and $\nabla\phi(\hat{\mathbf{n}})$ is the lensing deflection angle for the CMB photons.

Taking the Fourier transform, as appropriate for a flat-sky, we write the lensed temperature anisotropy in Fourier space as

$$\begin{aligned}\tilde{\Theta}(\boldsymbol{l}_1) &= \int d\hat{\mathbf{n}}\, \tilde{\Theta}(\hat{\mathbf{n}})e^{-i\boldsymbol{l}_1\cdot\hat{\mathbf{n}}} \\ &= \Theta(\boldsymbol{l}_1) - \int \frac{d^2\boldsymbol{l}_1'}{(2\pi)^2}\Theta(\boldsymbol{l}_1')L(\boldsymbol{l}_1, \boldsymbol{l}_1'),\end{aligned} \tag{19}$$

where

$$\begin{aligned}L(\boldsymbol{l}_1, \boldsymbol{l}_1') &\equiv \phi(\boldsymbol{l}_1 - \boldsymbol{l}_1')(\boldsymbol{l}_1 - \boldsymbol{l}_1')\cdot\boldsymbol{l}_1' \\ &\quad - \frac{1}{2}\int \frac{d^2\boldsymbol{l}_1''}{(2\pi)^2}\phi(\boldsymbol{l}_1'')\phi(\boldsymbol{l}_1 - \boldsymbol{l}_1' - \boldsymbol{l}_1'')(\boldsymbol{l}_1''\cdot\boldsymbol{l}_1') \\ &\quad \times(\boldsymbol{l}_1 - \boldsymbol{l}_1' - \boldsymbol{l}_1'')\cdot\boldsymbol{l}_1'\end{aligned} \tag{20}$$

to the second order in lensing potential in the perturbative expansion.

The observed angular power spectrum of CMB anisotropies under weak lensing is discussed in [3]. The resulting power spectrum consists of both the unlensed intensity and a perturbative correction related to the lensing effect. Making use of the expansion and after some straightforward calculations, we obtain the lensed anisotropy power spectrum as

$$\tilde{C}_l^\Theta = C_l^\Theta(1 - l^2R) + \int \frac{d^2\boldsymbol{l}_1}{(2\pi)^2}C_{l_1}^\phi C_{|\boldsymbol{l}-\boldsymbol{l}_1|}^\Theta[(\boldsymbol{l} - \boldsymbol{l}_1)\cdot\boldsymbol{l}_1]^2, \tag{21}$$

where

$$R = \frac{1}{4\pi}\int dl l^3 C_l^\phi. \tag{22}$$

Here, R describes the variance of the deflection angle. For ΛCDM cosmology, $\theta_{\rm rms} = \sqrt{R} \sim 2.6'$. This derivation makes use of the flat-sky approximation to describe the

lensing effect on CMB anisotropy power spectrum. When the expressions derived in the previous section for C_l^Θ and C_l^ϕ under the exact spherical-sky treatment are used in Eq. (21), the lensed CMB power spectrum can be derived with a less bias than using, say, the flat-sky result for C_l^ϕ in the same expression [3].

Keeping the flat-sky approximation, we can define the angular bispectrum as

$$\langle\Theta(\boldsymbol{l}_1)\Theta(\boldsymbol{l}_2)\Theta(\boldsymbol{l}_3)\rangle \equiv (2\pi)^2\delta(\boldsymbol{l}_1+\boldsymbol{l}_2+\boldsymbol{l}_3)B^\Theta_{(l_1,l_2,l_3)}, \quad (23)$$

and following the approach similar to the lensed angular power spectrum that led to Eq. (21), the lensed bispectrum can be expressed as

$$\begin{aligned}\tilde{B}^\Theta_{(l_1,l_2,l_3)} &= B^\Theta_{(l_1,l_2,l_3)}\left[1-(l_1^2+l_2^2+l_3^2)\frac{R}{2}\right]\\ &+\int\frac{d^2\mathbf{l}'}{(2\pi)^2}C^\phi_{l'}[B^\Theta_{(l_1,l_2-l',l_3+l')}(\boldsymbol{l}_2-\boldsymbol{l}')\\ &\cdot\boldsymbol{l}'(\boldsymbol{l}_1\text{-}+\boldsymbol{l}_2-\boldsymbol{l}')\cdot\boldsymbol{l}'+B^\Theta_{(l_1-l',l_2+l',l_3)}(\boldsymbol{l}_1-\boldsymbol{l}')\\ &\cdot\boldsymbol{l}'(\boldsymbol{l}_3+\boldsymbol{l}_1-\boldsymbol{l}')\cdot\boldsymbol{l}'+B^\Theta_{(l_1+l',l_2,l_3-l')}(\boldsymbol{l}_3-\boldsymbol{l}')\\ &\cdot\boldsymbol{l}'(\boldsymbol{l}_3+\boldsymbol{l}_2-\boldsymbol{l}')\cdot\boldsymbol{l}'].\end{aligned} \quad (24)$$

Note that we have identified the flat-sky bispectrum as $B^\Theta_{(l,l,l)321}$ to distinguish from the all-sky bispectrum $B^\Theta_{l_1,l_2,l_3}$. The two are related through

$$\begin{aligned}B^\Theta_{l_1l_2l_3} &= \begin{pmatrix}l_1 & l_2 & l_3\\ 0 & 0 & 0\end{pmatrix}\\ &\times\sqrt{\frac{(2l_1+1)(2l_2+1)(2l_3+1)}{4\pi}}B^\Theta_{(l_1,l_2,l_3)}\end{aligned} \quad (25)$$

B. All-sky treatment

The derivation related to the lensing of the CMB bispectrum under the more appropriate spherical sky can be obtained by replacing the Fourier components with spherical harmonic multipole moments. In this case, the lensed field can be represented as [3]

$$\begin{aligned}\tilde{\Theta}_{lm} &\approx \Theta_{lm}+\int d\hat{\mathbf{n}}\,Y_l^{m*}\nabla_i\phi(\hat{\mathbf{n}})\nabla^i\Theta(\hat{\mathbf{n}})\\ &+\frac{1}{2}\int d\hat{\mathbf{n}}\,Y_l^{m*}\nabla_i\phi(\hat{\mathbf{n}})\nabla_j\phi(\hat{\mathbf{n}})\nabla^i\nabla^j\Theta(\hat{\mathbf{n}})\\ &= \Theta_{lm}+\sum_{l'm'}\sum_{l''m''}\phi_{l'm'}\Theta_{l''m''}\\ &\times\left[I^{mm'm''}_{ll'l''}+\frac{1}{2}\sum_{l'''m'''}\phi^*_{l'''m'''}J^{mm'm''m'''}_{ll'l''l'''}\right],\end{aligned} \quad (26)$$

where, the integrals over the spherical harmonics were replaced, in the last step, by the geometrical factors

$$\begin{aligned}I^{mm'm''}_{ll'l''} &= \int d\hat{\mathbf{n}}\,Y_l^{m*}(\nabla_iY_{l'}^{m'})(\nabla^iY_{l''}^{m''}),\\ J^{mm'm''m'''}_{ll'l''l'''} &= \int d\hat{\mathbf{n}}\,Y_l^{m*}(\nabla_iY_{l'}^{m'})(\nabla_jY_{l'''}^{m'''*})\nabla^i\nabla^jY_{l''}^{m''}.\end{aligned} \quad (27)$$

Using Eq. (2), the lensed CMB temperature bispectrum can then be expressed as

$$\tilde{B}^{\ \Theta}_{l_1l_2l_3} = \sum_{m_1m_2m_3}\begin{pmatrix}l_1 & l_2 & l_3\\ m_1 & m_2 & m_3\end{pmatrix}\langle\tilde{\Theta}_{l_1m_1}\tilde{\Theta}_{l_2m_2}\tilde{\Theta}_{l_3m_3}\rangle, \quad (28)$$

leading to

$$\begin{aligned}\tilde{B}^\Theta_{l_1l_2l_3} &= \sum_{m_1m_2m_3}\begin{pmatrix}l_1 & l_2 & l_3\\ m_1 & m_2 & m_3\end{pmatrix}\Big[\langle\Theta_{l_1m_1}\Theta_{l_2m_2}\Theta_{l_3m_3}\rangle+\frac{1}{2}\sum_{l'_3m'_3}\sum_{l''_3m''_3}\sum_{l'''_3m'''_3}\langle\Theta_{l_1m_1}\Theta_{l_2m_2}\Theta_{l''_3m''_3}\phi_{l'_3m'_3}\phi^*_{l'''_3m'''_3}\rangle J^{m_3m'_3m''_3m'''_3}_{l_3l'_3l''_3l'''_3}+2\text{Perm}\\ &+\sum_{l'_2m'_2}\sum_{l''_2m''_2}\sum_{l'_3m'_3}\sum_{l''_3m''_3}\langle\Theta_{l_1m_1}\Theta_{l''_2m''_2}\Theta_{l''_3m''_3}\phi_{l'_2m'_2}\phi_{l'_3m'_3}\rangle I^{m_2m'_2m''_2}_{l_2l'_2l''_2}I^{m_3m'_3m''_3}_{l_3l'_3l''_3}+2\text{Perm}\Big].\end{aligned} \quad (29)$$

Noting that the Wigner-3j symbol obeys the identity

$$\sum_{m_1m_2}\begin{pmatrix}l_1 & l_2 & l_3\\ m_1 & m_2 & m_3\end{pmatrix}\begin{pmatrix}l_1 & l_2 & l''_3\\ m_1 & m_2 & m''_3\end{pmatrix} = \frac{\delta_{l_3l''_3}\delta_{m_3m''_3}}{(2l_3+1)}, \quad (30)$$

we can rewrite the lensed bispectrum as

$$\begin{aligned}\tilde{B}^{\ \Theta}_{l_1l_2l_3} &= B^\Theta_{l_1l_2l_3}+\frac{1}{2}B^\Theta_{l_1l_2l_3}\sum_{l'_3}C^\phi_{l'_3}S_1+2\text{Perm}\\ &+\sum_{l''_2l''_3}B^\Theta_{l_1l''_2l''_3}\sum_{l'_2}C^\phi_{l'_2}S_2+2\text{Perm}\end{aligned} \quad (31)$$

where

$$\begin{aligned}S_1 &= \frac{1}{(2l_3+1)}\sum_{m_3}\sum_{m'_3}J^{m_3m'_3m_3m'_3}_{l_3l'_3l_3l'_3}, \quad \text{and}\\ S_2 &= \sum_{m'_2m''_2m''_3}\sum_{m_1m_2m_3}\begin{pmatrix}l_1 & l_2 & l_3\\ m_1 & m_2 & m_3\end{pmatrix}\begin{pmatrix}l_1 & l''_2 & l''_3\\ m_1 & m''_2 & m''_3\end{pmatrix}\\ &\times I^{m_2m'_2m''_2}_{l_2l'_2l''_2}I^{m_3m'_2m''_3}_{l_3l'_2l''_3}\end{aligned} \quad (32)$$

The sum of the geometric term $J^{m_3m'_3m_3m'_3}_{l_3l'_3l_3l'_3}$ over m'_3 yields [3]

$$S_1 = -\frac{1}{(2l_3+1)}\sum_{m_3}\frac{1}{2}l_3(l_3+1)l'_3(l'_3+1)\frac{2l'_3+1}{4\pi}. \quad (33)$$

Hence, with summation over m_3 leading to a factor $(2l_3 + 1)$, the expression for S_1 simplifies to

$$S_1 = -\frac{1}{2} l_3(l_3+1) l_3'(l_3'+1) \frac{2l_3'+1}{4\pi}. \tag{34}$$

In order to evaluate S_2, we first reexpress $I^{mm'm''}_{ll'l''}$ as

$$I^{mm'm''}_{ll'l''} = f_{ll'l''} \begin{pmatrix} l & l' & l'' \\ m & m' & m'' \end{pmatrix}, \tag{35}$$

where [3]

$$f_{ll'l''} = \frac{1}{2}[l'(l'+1) + l''(l''+1) - l(l+1)] \begin{pmatrix} l & l' & l'' \\ 0 & 0 & 0 \end{pmatrix}. \tag{36}$$

Then the expression for S_2 can be rewritten as

$$\begin{aligned} S_2 &= f_{l_2 l_2' l_2''} f_{l_3 l_2' l_3''} \sum_{m_2' m_2'' m_3''} \sum_{m_1 m_2 m_3} \begin{pmatrix} l_1 & l_2 & l_3 \\ m_1 & m_2 & m_3 \end{pmatrix} \\ &\times \begin{pmatrix} l_1 & l_2'' & l_3'' \\ m_1 & m_2'' & m_3'' \end{pmatrix} \begin{pmatrix} l_2 & l_2' & l_2'' \\ m_2 & m_2' & m_2'' \end{pmatrix} \\ &\times \begin{pmatrix} l_3 & l_2' & l_3'' \\ m_3 & m_2' & m_3'' \end{pmatrix} \\ &= f_{l_2 l_2' l_2''} f_{l_3 l_2' l_3''} (-1)^{l'+l_2'+l_3'} \begin{Bmatrix} l_1 & l_2 & l_3 \\ l_2' & l_3'' & l_2'' \end{Bmatrix}, \end{aligned} \tag{37}$$

where, in the last step, we have introduced the Wigner-6j symbol [35]. The values of the Wigner-6j symbol can be computed numerically with a fast and efficient recursive algorithm [36].

Finally, substituting the expressions for S_1 and S_2 in Eq. (31) and including all permutations in a single expression, we can write the lensed bispectrum as

$$\begin{aligned} \tilde{B}^{\Theta}_{l_1 l_2 l_3} &= [1 - \mathcal{R}\{l_1(l_1+1) + l_2(l_2+1) + l_3(l_3+1)\}] B^{\Theta}_{l_1 l_2 l_3} + \sum_{lpq} C_l^{\phi\phi} \Big[f_{l_2 lp} f_{l_3 lq} (-1)^n \\ &\times \begin{Bmatrix} l_1 & l_2 & l_3 \\ l & q & p \end{Bmatrix} B^{\Theta}_{l_1 pq} f_{l_3 lp} f_{l_1 lq} (-1)^n \\ &\times \begin{Bmatrix} l_1 & l_2 & l_3 \\ p & l & q \end{Bmatrix} B^{\Theta}_{pl_2 q} f_{l_1 lp} f_{l_2 lq} (-1)^n \\ &\times \begin{Bmatrix} l_1 & l_2 & l_3 \\ q & p & l \end{Bmatrix} B^{\Theta}_{pql_3} \Big] \end{aligned}$$

where

$$\mathcal{R} = \frac{1}{4} \sum_l l(l+1) \frac{2l+1}{4\pi} C_l^{\phi\phi} \tag{38}$$

and $n \equiv (l + p + q)$.

V. RESULTS AND DISCUSSION

We illustrate the modification to the equilateral configurations of the bispectrum in Fig. 1, where we plot

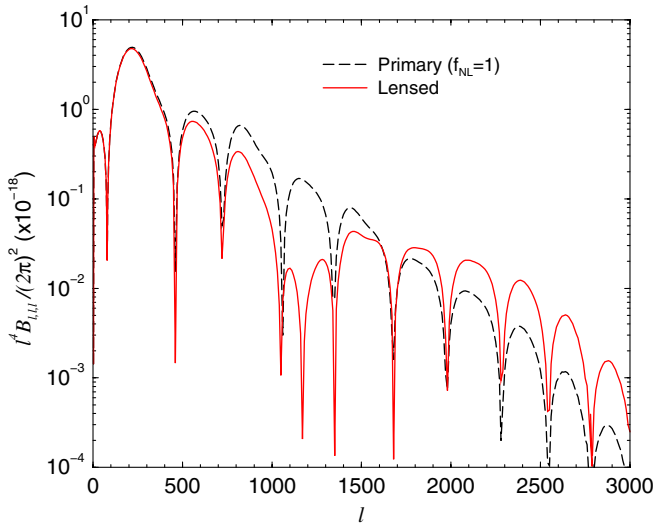

FIG. 1 (color online). The CMB bispectrum for the equilateral case $(l_1 = l_2 = l_3 = l)$ with (solid line) and without (dashed line) lensing. Here we plot $l^4 B^{\theta}_{lll}/(2\pi)^2$ as a function of the multipole l for one of the sides. We assume $f_{\rm NL} = 1$. The lensing effect can be described as a decrease in the amplitude of the bispectrum when $l \lesssim 1700$ with an increase at higher multipoles.

$l^4 B^{\Theta}_{lll}/(2\pi)^2$ as a function of the multipole l. The primary CMB bispectrum assumes $f_{\rm NL} = 1$ and is calculated with the full radiation transfer function $g_{Tl}(k)$. The lensing description makes use of the all-sky treatment to calculate both C_l^{ϕ} and the lensed bispectrum. The flat-sky expression gives a result consistent with the all-sky expression at better than 5% at all multipoles if the all-sky expression for C_l^{ϕ} is used in both calculations. The difference is at the level of 10% if the two expression make use of the two separate calculations of C_l^{ϕ}, as in the case of the angular power spectrum [3]. In the case of the equilateral configurations of the bispectrum, the lensing effect can be best described as a smoothing and a decrease of the amplitude of non-Gaussianity power in the equilateral configuration of the bispectrum when $l < 1500$ and a subsequent increase in the bispectrum amplitude at small angular scales.

In Fig. 2, we show two squeezed configurations ($l_1 \sim l_3 \gg l_2$) of the bispectrum, with the short length fixed at either 10 (left panel) or 100 (right panel), as a function of the multipole l of one side with the third side fixed at either $l + 10$ or $l + 100$. Without lensing, a comparison of Fig. 1 and 2 reveals a well-known result in the literature that the local type of the CMB bispectrum is dominated by squeezed configurations with one small side and two large sides for the bispectrum mode shape in the multipole space. With lensing, the amplitude of the squeezed configurations is significantly reduced when two of the sides have lengths $l > 1200$ in the multipole space. This can be again described as a smoothing effect with lensing by the intervening large-scale structure; removing or "washing

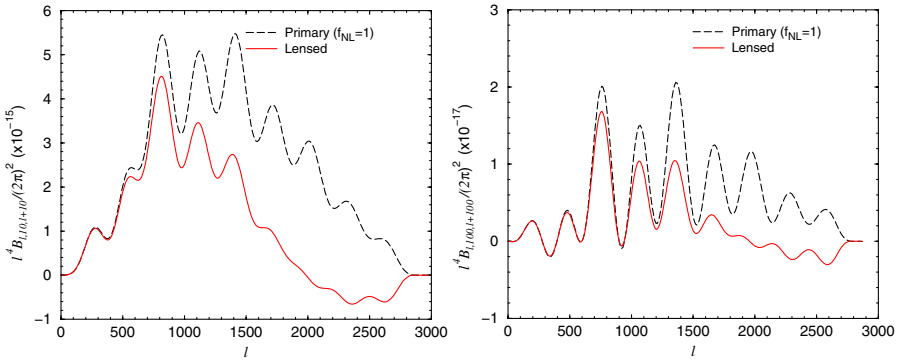

FIG. 2 (color online). The squeezed configurations ($l_1 \sim l_3 \gg l_2$) of the CMB bispectrum with (solid line) and without (dashed line) lensing. The left panel is for $l_2 = 10$ and right panel is $l_2 = 100$. We vary $l = l_1$ with $l_3 = l + l_2$ in both cases and plot $l^4 B_{l,l_2,l+l_2}/(2\pi)^2$ as a function of l. Again, we take $f_{\rm NL} = 1$. In these configurations, the lensing effect can be described as an overall decrease in the amplitude of the bispectrum when $l \lesssim 1200$. This suggests that lensing by the intervening large-scale structure leads to a less non-Gaussianity in the CMB map.

out'' the primordial non-Gaussian signature in the CMB map at angular scales below a few arcminutes. Thus, when lensed by the large-scale structure, the primordial non-Gaussian CMB sky appears more Gaussian at arcminute scales when studying the non-Gaussianity at the three-point level. At same angular scales, however, the CMB sky appears more non-Gaussian due to lensing at the four-point level probed by the trispectrum [35].

The removal of the non-Gaussianity is associated with the squeezed configurations, which dominate the overall signal-to-noise ratio for the detection of the primary bispectrum without lensing. Although non-Gaussianity is reduced for the squeezed configurations, lensing leads to an increase in the amplitude of the bispectrum for equilateral configurations where $l_1 \sim l_2 \sim l_3 > 1500$. This increase, however, is insignificant in terms of the overall signal-to-noise ratio as the contribution to the cumulative signal-to-noise coming from these configurations is lower, owing to the higher variances associated with foregrounds and instrumental noise at these angular scales.

To further quantify this statement, we plot, in Fig. 3, the signal-to-noise ratio calculated as

$$\left(\frac{S}{N}\right)^2 = \sum_{l_1 l_2 l_3} \frac{(B^{\Theta}_{l_1 l_2 l_3})^2}{6 C^{\rm tot}_{l_1} C^{\rm tot}_{l_2} C^{\rm tot}_{l_3}}, \tag{39}$$

where the noise variance calculation involves all contributions to the angular power spectrum with $C^{\rm tot}_l = \tilde{C}_l + C^{\rm sec}_l + N_l$ where we include the lensed CMB power spectrum ($\tilde{C}_l$), secondary anisotropies ($C^{\rm sec}_l$), and the noise power spectrum (N_l) for both WMAP and Planck. For secondaries, we include the SZ power spectrum calculated with the halo model [37] and make use of the noise calculations from Ref. [26] for WMAP and Planck. For the case involving an experiment limited by the cosmic variance, we set $N_l = 0$. In the left panel of Fig. 3, we plot $d(S/N)^2/dl_3$ as a function of l_3, while in the right panel we plot the cumulative signal-to-noise ratio out to l_3 in the x-axis. In the case where lensing is not included, signal-to-

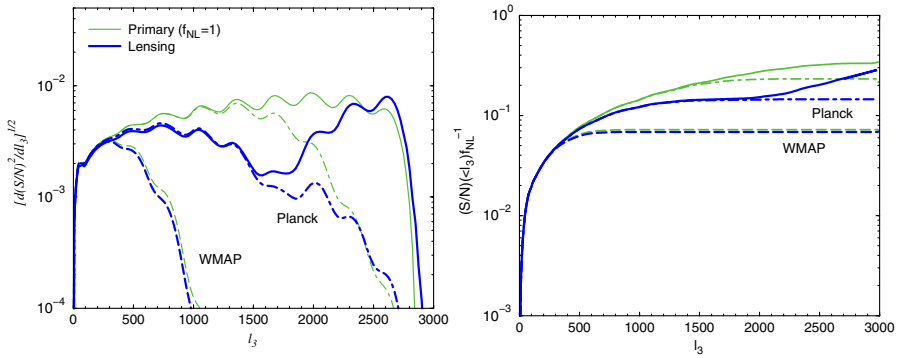

FIG. 3 (color online). The signal-to-noise ratio for a detection of the CMB bispectrum with (thick lines) and without (thin lines) lensing. The long-dashed lines show the case for WMAP and dot-dashed lines for Planck. The left panel shows the signal-to-noise ratio as a function of l_3, while the right panel shows the cumulative signal-to-noise ratio below l_3 in the x-axis. Note the overall reduction in the signal-to-noise ratio (when $l_3 \sim 1500$) in the case of lensing relative to the case where lensing is ignored.

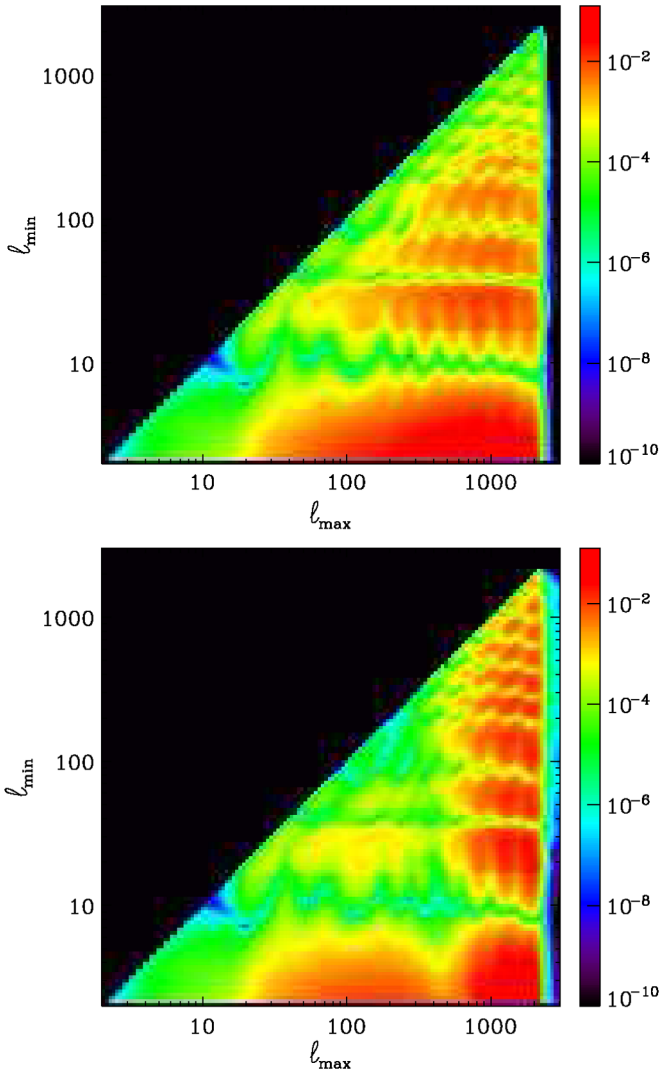

FIG. 4 (color online). Contour plots of $d(S/N)^2/d\log l_{\rm max} d\log l_{\rm min}$ [Eq. (40)] as a function of $l_{\rm max}$ and $l_{\rm min}$ for the primary bispectrum (top panel) and the lensed primary bispectrum (bottom panel). We take $f_{\rm NL} = 1$.

noise ratio estimates for the bispectrum detection are consistent with previous calculations in the literature [10].

With lensing, however, the signal-to-noise ratios are changed. As can be seen from the left panel of Fig. 3, there is an overall reduction in the signal-to-noise ratio when $l_3 \sim 1500$. This difference comes from the previously described decrease in the amplitude of the non-Gaussianity in squeezed configurations of the bispectrum with lensing imposed. To further understand the differences in the signal-to-noise ratio of the lensed primary bispectrum, we plot, in Fig. 4, the quantity

$$\frac{d(S/N)^2}{d\log l_{\rm max} d\log l_{\rm min}} = l_{\rm max} l_{\rm min} \sum_{l=l_{\rm min}}^{l_{\rm max}} \frac{(B^{\Theta}_{l_{\rm min} l l_{\rm max}})^2}{6 C^{\rm tot}_{l_{\rm min}} C^{\rm tot}_{l} C^{\rm tot}_{l_{\rm max}}}, \quad (40)$$

with two separate estimates for B^{Θ} and $\tilde{B}^{\Theta}$ to estimate this quantity without and with lensing, respectively. Note that the overall signal-to-noise ratio comes from integrating this quantity over the variables $l_{\rm max}$ and $l_{\rm min}$ and we include the factor $l_{\rm max} l_{\rm min}$ to account for the logarithmic scaling. A comparison of the two panels in Fig. 4 reveals an overall decrease in the amplitude at $l \sim 10^3$ in the case with the lensed primary bispectrum relative to the primary bispectrum alone.

In Fig. 5, we plot the difference of the two as a contour plot to show that lensing results in an overall decrease in the signal-to-noise ratio in the squeezed configurations when $l_{\rm max} \sim 10^3$ and $l_{\rm min} < 10^2$, while there is an increase in the signal-to-noise ratio when $l_{\rm max} \sim 3 \times 10^3$ for all values of $l_{\rm min}$. These plots demonstrates the same trends described with respect to Fig. 2 involving a decrease in the amplitude of the squeezed configurations of the lensed bispectrum. While there is a slight increase in the lensed bispectrum amplitude at $l_3 > 2000$, such small angular scales are not probed by Planck. Even in the cosmic variance limit, unfortunately, this small increase is insignificant given that at these same angular scales secondary anisotropies dominate the bispectrum noise variance. In terms of the cumulative signal-to-noise ratio values shown in Fig. 3, the minimum $f_{\rm NL}$ to detect the bispectrum with Planck and a cosmic variance-limited experiment is increased by about 30% to 40% from $f_{\rm NL} \sim 5$ for Planck to $f_{\rm NL} \sim 7$. The cosmic variance-limited detection threshold for $f_{\rm NL}$ is increased from 3 to 5.

While the difference in cumulative signal-to-noise ratio seems insignificant for an experiment like WMAP, weak lensing could impact existing measurements of the non-Gaussianity parameter $f_{\rm NL}$ [13,14]. To understand the lensing bias introduced to $f_{\rm NL}$, we follow the discussion

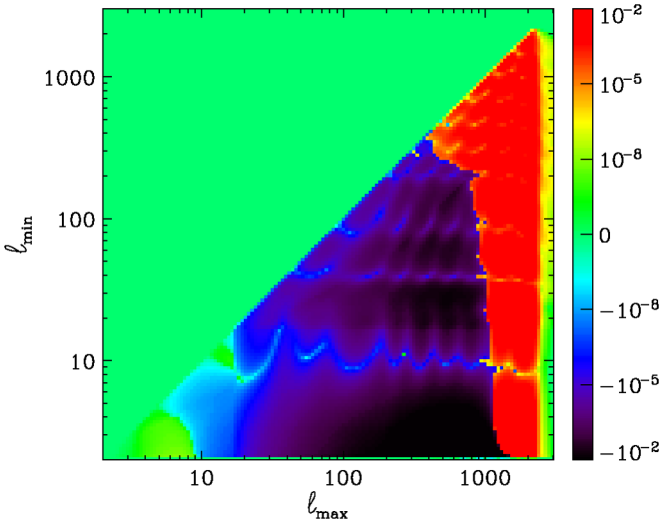

FIG. 5 (color online). Contour plot of the difference $d[(S/N)^2_{\rm lensed} - (S/N)^2_{\rm unlensed})/d\log l_{\rm max} d\log l_{\rm min}$ as a function of $l_{\rm max}$ and $l_{\rm min}$ (same as the difference between bottom and top panels of Fig. 4).

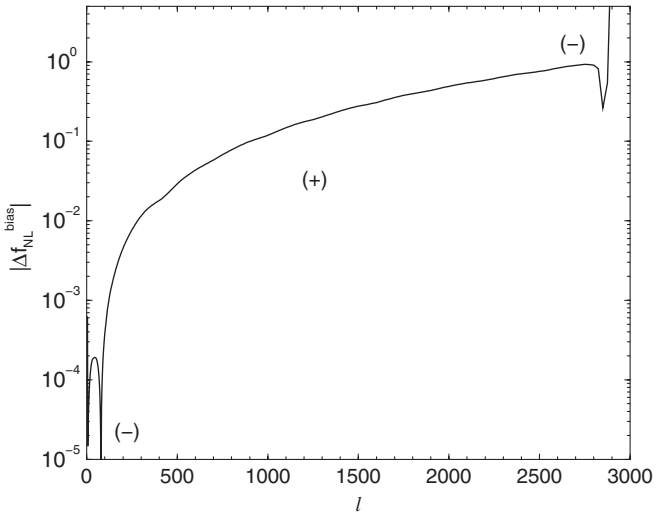

FIG. 6. The bias in the primordial non-Gaussianity parameter $f_{\rm NL}$ when lensing is ignored in the estimation. $(+)/(-)$ shows the sign of $\Delta f_{\rm NL}/f_{\rm NL}$ between the true and measured values (see text for details).

in Ref. [28] and note that the current estimators of the non-Gaussianity parameter use $\hat{f}_{\rm NL} = \frac{\hat{S}_{\rm prim}}{N}$ [30,38,39], with

$$\hat{S}_{\rm prim} = \sum_{\mathbf{pq}} B^{\Theta}_{l_1 l_2 l_3} \mathcal{C}^{-1}_{\mathbf{pq}} \hat{B}^{\rm obs}_{l'_1 l'_2 l'_3} \tag{41}$$

where $B^{\Theta}_{l_1 l_2 l_3}$ is the primary bispectrum, and $\mathcal{C}_{\mathbf{pq}}$ is the covariance matrix for bispectrum measurements involving triplets of $\mathbf{p} \equiv (l_1 l_2 l_3)$ and $\mathbf{q} \equiv (l'_1 l'_2 l'_3)$. This estimator is the optimal estimator for non-Gaussianity measurements, but given the complications associated with estimating the covariance, existing studies make use of a suboptimal estimator which approximates the covariance with variance $\mathcal{C}^{-1}_{\alpha\alpha'} \approx \sigma^{-2}(l_1, l_2, l_3)\delta_{\alpha\alpha'}$, and introduces a linear term to Eq. (41) to minimize the variance of $\hat{f}_{\rm NL}$ [39]. Note that N is the overall normalization factor that can be calculated from Eq. (41) by replacing $\hat{B}^{\rm obs}$ with B^{Θ}.

While weak lensing modifies the observed bispectrum $\hat{B}^{\rm obs}_{l_1 l_2 l_3} = f_{\rm NL} \tilde{B}^{\Theta}_{l_1 l_2 l_3}$, existing measurements make the assumption that $\hat{B}^{\rm obs}_{l_1 l_2 l_3} = f_{\rm NL} B^{\Theta}_{l_1 l_2 l_3}$. This results in a biased estimate of $\hat{f}_{\rm NL}$ from the true value of the non-Gaussianity parameter $f^{\rm true}_{\rm NL}$. The fractional difference of this bias $\Delta f/\hat{f}_{\rm NL} \equiv (f^{\rm true}_{\rm NL} - \hat{f}_{\rm NL})/\hat{f}_{\rm NL}$ can be calculated through the covariance between the lensed and unlensed CMB primary bispectrum $\Delta f/\hat{f}_{\rm NL} = 1 - [\sum B^{\Theta}_{l_1 l_2 l_3} \sigma^{-2} \tilde{B}^{\Theta}_{l_1 l_2 l_3} / \sum B^{\Theta}_{l_1 l_2 l_3} \sigma^{-2} B^{\Theta}_{l_1 l_2 l_3}]$, where we have simply written the variance as σ^{-2}. We plot $\Delta f/\hat{f}_{\rm NL}$ as a function of l to which non-Gaussianity parameter measurements are performed in Fig. 6. Existing measurements with WMAP data probe out to $l_{\rm max} \sim 750$ and we find that existing estimates of $f_{\rm NL}$ are biased by $\sim$6%. For Planck, if lensing is ignored, the bias is at the level of 30%.

This bias is not the same fractional difference in the signal-to-noise ratio that one can infer from Fig. 3 since the fractional difference in the signal-to-noise ratio with and without lensing involves a ratio of the form $[\sum \tilde{B}^{\Theta}_{l_1 l_2 l_3} \sigma^{-2} \tilde{B}^{\Theta}_{l_1 l_2 l_3} / \sum B^{\Theta}_{l_1 l_2 l_3} \sigma^{-2} B^{\Theta}_{l_1 l_2 l_3}]$. Note that in future an unbiased estimate of $f_{\rm NL}$ can be obtained by replacing $B^{\Theta}_{l_1 l_2 l_3}$ in Eq. (41) with the lensed bispectrum $\tilde{B}^{\Theta}_{l_1 l_2 l_3}$ and recalculating the normalization factor N with the lensed primary bispectrum. Unfortunately, while without lensing the CMB primary bispectrum of the local model factorizes into two separate integrals with b^L_l and $b^{\rm NL}_l$ (described in Sec. II), this factorizability is no longer preserved when lensed and impacts an easy estimation of the non-Gaussianity parameter with the existing estimator [30]. For Planck and other CMB experiments that can probe down to small angular scales for primordial non-Gaussianity measurements, it will be necessary to implement an estimator that accounts for the lensing effect.

To summarize the main results of this paper, we have discussed the primary CMB bispectrum generated at the last scattering surface, but observed today after it is weak lensed by the intervening large-scale structure. Unfortunately, as we have found, weak lensing leads to an overall decrease in the amplitude of non-Gaussianity with the biggest change on the squeezed configurations of the bispectrum that dominate the overall signal-to-noise ratio when studying the primordial non-Gaussianity parameter. For an experiment such as the Wilkinson Microwave Anisotropy Probe (WMAP), the modifications imposed by lensing results in an estimate of $f_{\rm NL}$ of the local model that is biased low by about 6%. For a high resolution experiment such as Planck, the lensing modification to the bispectrum must be accounted for when attempting to estimate the primordial non-Gaussianity. The minimum detectable value of $f_{\rm NL}$ for a cosmic variance limited experiment is $\sim$5.

ACKNOWLEDGMENTS

We thank participants of the recent non-Gaussianity workshop at the Perimeter Institute for helpful discussions and Alex Amblard for help with Fig. 4. P. S. thanks Tommaso Stasi. This work was supported by NSF CAREER AST-0645427. We acknowledge the use of CMBFAST by Uros Seljak and Matias Zaldarriaga [31].

[1] See, e.g., U. Seljak and M. Zaldarriaga, Phys. Rev. Lett. **82**, 2636 (1999); Phys. Rev. D **60**, 043504 (1999); M. Zaldarriaga and U. Seljak, Phys. Rev. D **59**, 123507 (1999); M. Zaldarriaga, Phys. Rev. D **62**, 063510 (2000); M. H. Kesden, A. Cooray, and M. Kamionkowski, Phys. Rev. D **66**, 083007 (2002); C. Vale, A. Amblard, and M. J. White, New Astron. Rev. **10**, 1 (2004); A. Amblard, C. Vale, and M. J. White, New Astron. Rev. **9**, 687 (2004); S. Das and P. Bode, arXiv:0711.3793.

[2] For a recent review see, A. Lewis and A. Challinor, Phys. Rep. **429**, 1 (2006).

[3] W. Hu, Phys. Rev. D **62**, 043007 (2000).

[4] W. Hu and T. Okamoto, Astrophys. J. **574**, 566 (2002); M. Kesden, A. Cooray, and M. Kamionkowski, Phys. Rev. D **67**, 123507 (2003); C. M. Hirata and U. Seljak, Phys. Rev. D **68**, 083002 (2003).

[5] M. Kamionkowski, A. Kosowsky, and A. Stebbins, Phys. Rev. Lett. **78**, 2058 (1997); U. Seljak and M. Zaldarriaga, Phys. Rev. Lett. **78**, 2054 (1997).

[6] M. Kesden, A. Cooray, and M. Kamionkowski, Phys. Rev. Lett. **89**, 011304 (2002); L. Knox and Y.-S. Song, Phys. Rev. Lett. 011303 **89**; U. Seljak and C. Hirata, Phys. Rev. D **69**, 043005 (2004).

[7] M. Zaldarriaga and U. Seljak, Phys. Rev. D **58**, 023003 (1998).

[8] K. M. Smith, O. Zahn, and O. Dore, Phys. Rev. D **76**, 043510 (2007).

[9] C. M. Hirata, S. Ho, N. Padmanabhan, U. Seljak, and N. Bahcall, arXiv:0801.0644.

[10] E. Komatsu and D. N. Spergel, Phys. Rev. D **63**, 063002 (2001).

[11] M. Liguori, F. K. Hansen, E. Komatsu, S. Matarrese, and A. Riotto, Phys. Rev. D **73**, 043505 (2006).

[12] E. Komatsu *et al.* (WMAP Collaboration), Astrophys. J. Suppl. Ser. **148**, 119 (2003).

[13] E. Komatsu *et al.* (WMAP Collaboration), arXiv:0803.0547.

[14] A. P. S. Yadav and B. D. Wandelt, Phys. Rev. Lett. **100**, 181301 (2008).

[15] D. S. Salopek and J. R. Bond, Phys. Rev. D **42**, 3936 (1990); **43**, 1005 (1991).

[16] T. Falk, R. Rangarajan, and M. Srednicki, Astrophys. J. **403**, L1 (1993).

[17] A. Gangui, F. Lucchin, S. Matarrese, and S. Mollerach, Astrophys. J. **430**, 447 (1994).

[18] T. Pyne and S. M. Carroll, Phys. Rev. D **53**, 2920 (1996).

[19] J. M. Maldacena, J. High Energy Phys. 05 (2003) 013.

[20] V. Acquaviva, N. Bartolo, S. Matarrese, and A. Riotto, Nucl. Phys. **B667**, 119 (2003).

[21] N. Bartolo, S. Matarrese, and A. Riotto, Phys. Rev. Lett. **93**, 231301 (2004).

[22] N. Bartolo, E. Komatsu, S. Matarrese, and A. Riotto, Phys. Rep. **402**, 103 (2004).

[23] E. I. Buchbinder, J. Khoury, and B. A. Ovrut, Phys. Rev. Lett. **100**, 171302 (2008).

[24] J. L. Lehners and P. J. Steinhardt, Phys. Rev. D **77**, 063533 (2008).

[25] D. M. Goldberg and D. N. Spergel, Phys. Rev. D **59**, 103002 (1999).

[26] A. R. Cooray and W. Hu, Astrophys. J. **534**, 533 (2000).

[27] K. M. Smith and M. Zaldarriaga, arXiv:astro-ph/0612571.

[28] P. Serra and A. Cooray, Phys. Rev. D **77**, 107305 (2008).

[29] D. Babich and E. Pierpaoli, arXiv:0803.1161.

[30] E. Komatsu, D. N. Spergel, and B. D. Wandelt, Astrophys. J. **634**, 14 (2005).

[31] U. Seljak and M. Zaldarriaga, Astrophys. J. **469**, 437 (1996).

[32] R. D. Blandford *et al.*, Mon. Not. R. Astron. Soc. **251**, 600 (1991); J. Miralda-Escudé, Astrophys. J. **380**, 1 (1991); N. Kaiser, Astrophys. J. **388**, 272 (1992); M. Bartelmann and P. Schneider, Astron. Astrophys. **259**, 413 (1992). For reviews, see, M. Bartelmann and P. Schneider, Phys. Rep. **340**, 291 (2001); P. Schneider, *Gravitational Lensing: Strong, Weak & Micro, Saas-Fee Advanced Course 33* (Springer-Verlag, Berlin, 2006).

[33] W. Hu and A. Cooray, Phys. Rev. D **63**, 023504 (2000).

[34] A. R. Cooray, New Astron. Rev. **9**, 173 (2004); A. Challinor and A. Lewis, Phys. Rev. D **71**, 103010 (2005).

[35] W. Hu, Phys. Rev. D **64**, 083005 (2001).

[36] K. Schulten and R. Gordon, J. Math. Phys. (N.Y.) **16**, 1971 (1975).

[37] A. Cooray and R. K. Sheth, Phys. Rep. **372**, 1 (2002); A. Cooray, Phys. Rev. D **62**, 103506 (2000).

[38] P. Creminelli, A. Nicolis, L Senatore, M. Tegmark, and M. Zaldarriaga, J. Cosmol. Astropart. Phys. 5, 4 (2006).

[39] A. P. S. Yadav, E. Komatsu, B. D. Wandelt, M. Liguori, F. K. Hansen, and S. Matarrese, arXiv:0711.4933.